



# Anodes for Carbon-Fueled Solid Oxide Fuel Cells

Wei Zhou,<sup>[a]</sup> Yong Jiao,<sup>[b]</sup> Si-Dian Li,<sup>[b]</sup> and Zongping Shao<sup>\*[a, c]</sup>

Solid oxide fuel cells (SOFCs) have been considered as one of the most promising technologies for high-efficiency electrical energy generation using a variety of fuels, including hydrogen, natural gas, biogas, carbon monoxide, liquid hydrocarbons and solid carbon. Carbon-fueled SOFCs (CF-SOFCs) potentially have the highest volume power density because solid carbon has a fuel energy density of 23.95 kWh L<sup>-1</sup>, which is approximately 10 times higher than that of liquid hydrogen. However, the re-

activity and fluid mobility of carbon is significantly lower than those of gaseous fuels; thus, CF-SOFCs will be kinetically limited at the anode. Herein, we review the development of anodes in CF-SOFCs from the perspective of material compositions and microstructures. Challenges and research trends based on the fundamental understanding of the materials science and engineering for anode development in CF-SOFCs are discussed.

## 1. Introduction

Fuel cells are devices that electrochemically convert the chemical energy present in a fuel into electrical energy and heat without combustion.<sup>[1–3]</sup> A fuel cell consists of an anode, a cathode, an electrolyte and interconnects. At the anode, fuel is oxidized and releases electrons. The electrons are collected by the interconnects, and then they travel through an external circuit to supply useful work and return to the cathode. The operating temperatures vary considerably (e.g., from room temperature to 1000 °C) for different types of fuel cells. Therefore, the materials and microstructure of the electrodes, electrolyte and other stack components vary significantly to fulfill the special requirements of different types of fuel cells.

Although hydrogen is often referred to as the ideal fuel of the future, there are a number of problems related to hydrogen generation and storage that must be overcome before it could be implemented on a wide scale. Most fuel cells must operate on hydrogen, which is one of the primary limitations of current fuel cell technologies. Solid oxide fuel cells (SOFCs) are one of the most promising types of fuel cells due to their fuel flexibility. Oxygen anions (O<sup>2-</sup>) are the species that are transported through the electrolyte of the SOFC, which allows the SOFC to operate on any combustible fuel, including hydro-

gen, natural gas, carbon monoxide, ammonia, methanol, dimethyl ether and even solid carbon.<sup>[4–10]</sup>

The anode materials and configurations of SOFCs vary with the types of fuel used. Conventional SOFCs use nickel-based cermet anodes, which exhibit high electrical conductivity, good compatibility with electrolytes, and high electrocatalytic activity toward the oxidation of hydrogen. However, because nickel-based anodes tend to experience carbon deposition in methane-rich fuels, carbon accumulation tends to occur on the anode, which leads to the rapid degradation of the fuel cell's performance. Many alternative materials have been developed to overcome this issue, which has been described in detail in the literature.<sup>[11–17]</sup>

Coal is the second largest primary energy source in the world after oil and is a major source of electricity generation when used in thermal power plants due to its abundance and low price.<sup>[18]</sup> Currently, coal-based electricity production accounts for more than 70% of the electricity produced in China and India, and 50% in the United States.<sup>[19]</sup> However, coal utilization technologies must continue to be improved due to the characteristics of coal-fired power plants, which include relatively low efficiencies, considerable greenhouse gas emissions, acid rain, and particulate and heavy metal pollution. Electrical power generation in SOFCs that directly utilize solid carbonaceous fuels would provide significant benefits including high energy-conversion efficiencies (i.e., thermodynamically near 100%), very pure CO<sub>2</sub> generation when using clean coal, and the possible usage of various types of carbon sources, including petroleum coke, coal coke, cracked biomass or pyrolyzed hydrocarbons.<sup>[20]</sup> Carbon-fueled SOFCs (CF-SOFCs) may also be able to use a given volume of fuel more efficiently. Solid carbon has a fuel energy density of 23.95 kWh L<sup>-1</sup> compared to that of diesel (10.6 kWh L<sup>-1</sup>), liquid methane (5.9 kWh L<sup>-1</sup>) and liquid hydrogen (2.6 kWh L<sup>-1</sup>).<sup>[21,22]</sup>

CF-SOFCs are also referred to as “direct carbon solid oxide fuel cells (DC-SOFCs),” “solid oxide direct carbon fuel cells (SO-DCFCs)” or “hybrid direct carbon fuel cells (HDCFCs)” in the lit-

[a] Prof. W. Zhou, Prof. Z. Shao  
State Key Laboratory of Materials-Oriented Chemical Engineering  
College of Chemistry & Chemical Engineering  
Nanjing University of Technology  
No. 5 Xin Mofan Road, Nanjing 210009 (PR China)  
address:  
E-mail: shaozp@njtech.edu.cn

[b] Prof. Y. Jiao, Prof. S.-D. Li  
Institute of Molecular Science  
Shanxi University  
No. 92 Wucheng Road, Taiyuan 030006 (PR China)

[c] Prof. Z. Shao  
College of Energy  
Nanjing University of Technology  
No. 5 Xin Mofan Road, Nanjing 210009 (PR China)

erature.<sup>[23–26]</sup> T. M. Gür<sup>[27]</sup> suggests that the word “direct” may lead to misunderstanding if not used in the proper context because “direct” electrochemical reactions of solid carbon with  $O^{2-}$  are difficult to achieve; in practice, carbon is provided as a gaseous fuel such as CO and  $H_2$  to the electrochemical reaction site or is converted by oxygen in the form of  $OH^-$ ,  $CO_3^{2-}$ , or a metal oxide. Therefore, we use CF-SOFCs in this paper to describe this family of fuel cells.

Many attempts have been pursued to develop a fuel cell that can use solid carbons as fuels for nearly 150 years since the first carbon fuel cell was made by Jacques in the 19th century.<sup>[28]</sup> Molten hydroxide was used in Jacques’s design. Hydroxide eutectics melt at significantly lower temperatures than their molten carbonate counterparts; this fact expands the operational regime of carbon fuel cells using hydroxide eutectics to lower temperatures. However, a critical problem with this type of fuel cell is the reaction of the hydroxide electrolyte with carbon to form carbonate. Weaver et al.<sup>[29]</sup> presented a molten carbonate electrolyte for direct carbon conversion in 1979. Solid carbon could be wetted by the eutectic molten carbonate, which increases the possibility of the electrochemical oxidation of carbon due to the enhanced active reaction area.<sup>[30]</sup> The primary technical challenge of this type cell is the corrosion of its electrodes and metal bipolar plates. Among the different types of carbon fuel cells, CF-SOFCs are believed to be the most promising due to their simple construction and maintenance requirements, which do not require the recycling of its anode or cathode gases. CF-SOFCs use a traditional oxide ion conductor, such as yttria-stabilized zirconia (YSZ), as an electrolyte, which separates the cathode and anode, reducing the possibility of cathode corrosion with carbonate.

The utilization of carbon as a fuel for SOFCs is at an early stage of development and will require considerable effort to make it commercially viable. The major technical issue with CF-SOFCs currently is the difficulty in transporting the solid fuel into the anode reaction zone or to the triple-phase boundaries (TPBs) using porous anodes. When using a gaseous fuel, fuel can easily be delivered through the porous structure of the anode to reach the fuel/anode/electrolyte triple junction reaction sites for its oxidation with migrating oxygen ions and electrons transfer to the anode. However, for a solid fuel, continuous fuel delivery to reaction sites is a significant challenge. Therefore, contact between the anode and the carbonaceous fuel has a strong effect on the CF-SOFC’s reaction characteristics. Other challenges include fuel processing and fuel quality requirements; understanding the electrochemical reaction kinetics and mechanism for carbon oxidation; corrosion of cell components, particularly where molten salts are used as the fuel carrier; improvement in materials performance, power densities and useful lifetimes; overall systems design; and technology upscaling. Some of these aspects have been reviewed, and we will not try to duplicate them in this paper.<sup>[20, 27, 31–35]</sup>

The key components of a CF-SOFC are similar to a gas-fueled SOFC and include a perovskite cathode, such as  $La_{1-x}Sr_xMnO_3$  (LSM) or  $La_{1-x}Sr_xCo_{1-y}Fe_yO_3$  (LSCF), a solid YSZ or  $Sm_{0.2}Ce_{0.8}O_{1.9}$  (SDC) electrolyte, and a cermet anode YSZ-Ni or

SDC-Ni. Differences between the various types of CF-SOFCs arise from the type of contact maintained between the anode and the carbon fuel. Solid carbon fuel could be directly in contact with a solid anode or carbon could be mixed with a molten metal or salt at the anode. A tree diagram of various CF-SOFCs is shown in Figure 1 to clarify the various technologies under development.

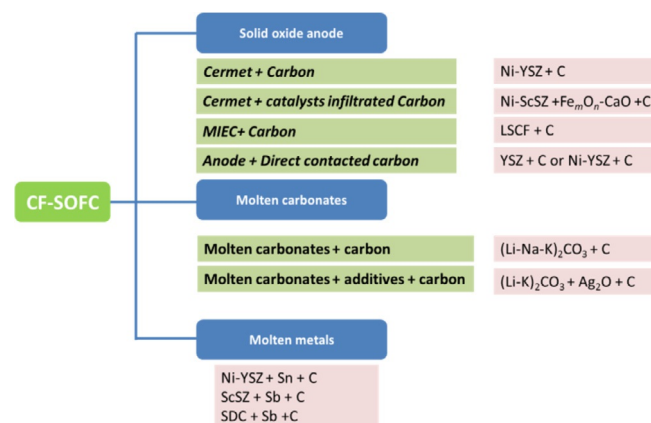


Figure 1. A tree diagram of CF-SOFCs with various anodes.

For a CF-SOFC power system, the power density and efficiency are critical performance parameters. Power density is related to the system size, portability, and cost. In certain applications, cost is more critical than portability and volume requirements. Improving power density reduces the size of the fuel cell system and thus its cost as well. Efficiency is a critical factor to differentiate CF-SOFCs from other types of fuel cells. The thermodynamic efficiency of CF-SOFCs marginally exceeds 100% nearly independently of the conversion temperature, which has the potential to far exceed the efficiencies of SOFCs using other fuels (Figure 2).<sup>[36]</sup> However, if this efficiency cannot be achieved, then CF-SOFCs will likely not be competitive with other fuel cell options. Herein, the various materials and structural designs of the anodes used in CF-SOFCs are reviewed in brief because these properties are closely related to

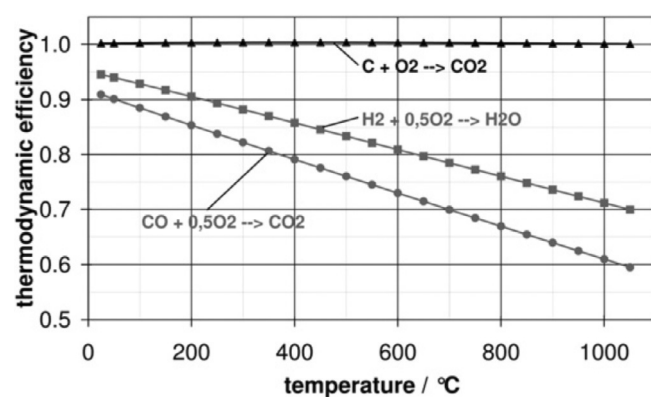


Figure 2. Thermodynamic efficiency as function of temperature for different reactions: carbon oxidation ▼; hydrogen oxidation ■; carbon monoxide oxidation ●.<sup>[36]</sup>

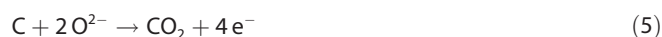
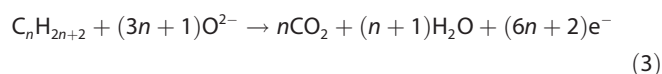
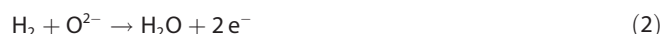
the power generation and efficiency of these types of fuel cells.

## 2. Principle of SOFCs Fed with Carbon

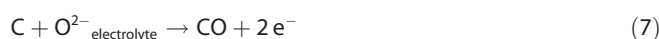
SOFCs are complex electrochemical devices that contain three basic components: a porous anode, an electrolyte membrane, and a porous cathode. The cathode is typically an oxide that catalyzes the oxygen reduction reaction [Reaction (1)]:



The anode catalyzes the oxidation of the fuel. The reactions can be different based on the fuel used [Reactions (2)–(5)]:



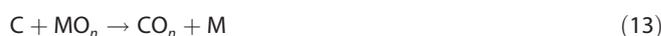
The thermodynamic efficiency of the complete electrochemical oxidation of solid carbon is greater than 100% because the Gibbs free energy of the reaction ( $\Delta G = -395.4 \text{ kJ mol}^{-1}$ ,  $\Delta G = \Delta H - T\Delta S$ ) is minimally higher than the enthalpy of the reaction ( $\Delta H = -394.0 \text{ kJ mol}^{-1}$ ) at  $600^\circ\text{C}$ ; this is due to the marginally positive entropy term ( $\Delta S = 1.6 \text{ JK}^{-1} \text{ mol}^{-1}$ , no entropic heat evolution) for the ideal fuel cell reaction ( $C + O_2 \rightleftharpoons CO_2$ ).<sup>[31]</sup> Because the entropy term is near zero, the thermodynamic efficiency of the oxidation of solid carbon via oxygen (i.e., a full-cell reaction) is also temperature-independent. Additionally, because the product of this reaction,  $CO_2$ , exists in a separate gas state, the progression of the reaction does not influence the activity of the solid carbon fuel, which is usually assumed to be equal to one.<sup>[36]</sup> This may allow a full conversion of the carbon fuel in a single step with the theoretical voltage of CF-SOFCs remaining nearly constant at approximately 1.02 V during the operation (i.e., minimal Nernst loss). However, the open-circuit voltages (OCVs) produced by CF-SOFCs differ from the theoretical value of carbon oxidation (i.e., 1.02 V) due to the difficulties of achieving direct oxidation of carbon. Compared to a hydrogen-fed fuel cell, which produces only a single product (i.e., water), carbon-fueled SOFCs produce two products: CO and  $CO_2$ . The reaction product distribution (i.e., the selectivity for either  $CO_2$  or CO) depends on the temperature and anode potential. In addition to the complete oxidation of the solid carbon reaction [Reaction (6)] being the most desirable reaction, other reactions including the incomplete oxidation of carbon [Reaction (7)], the oxidation of CO [Reaction (8)], and the Boudouard reaction [Reaction (9)] may also occur in the anode chamber.<sup>[33]</sup>



Molten carbonates have high ionic conductivities, which are used in the anode to catalyze and add additional reaction sites for carbon oxidation. Carbon fuel is typically supplied in the form of fine particles that are mixed with a molten carbonate electrolyte. The reactions that occur at the anode are more complex. In addition to Reactions (6)–(9), additional reactions may also occur at the anode [Reactions (10) and (11)]:



Maintaining percolation and sufficient electrical connectivity among the carbon particles in the molten carbonate electrolyte at all times is a critical operational challenge. This problem can be eliminated entirely when an electronically conductive molten metal anode is used to ensure excellent conductivity among the dispersed carbon particles in the melt. The basic operating principle of this system can be represented by the reactions of the metal, M, at the anode [Reactions (12) and (13)]:



## 3. Materials and Structural Development of the Anode in CF-SOFCs

### 3.1. Solid Oxide Anode

#### 3.1.1. Cermet + Carbon

Ni-based cermet materials, such as Ni/YSZ and Ni/SDC, are the most common anodes used in SOFCs. The Ni in the cermet anode provides electronic conductivity and catalytic activity for the oxidation of hydrogen. The YSZ or doped  $CeO_2$  provides a thermal expansion match with the electrolyte, ionic conductivity to extend the reaction zone in the anode, and structural support for the anode that prevents Ni sintering. Ni-based cermet materials have also been used as anodes in CF-SOFCs with different configurations, including electrolyte-supported, anode-supported and cathode-supported fuel cells in tubular or planar geometries.

The possibility of converting solid carbonaceous fuels to electricity in a fluidized bed CF-SOFC arrangement was first proposed by Gür and Huggins in 1992.<sup>[37]</sup> The solid carbon was added in a tubular, YSZ-supported SOFC that used porous Pt as its cathode and anode; the power density was only  $4.2 \text{ mW cm}^{-2}$  at 0.6 V and  $955^\circ\text{C}$ . Later, those researchers used Ni/YSZ cermet anodes to improve the performance of the anode.<sup>[38]</sup> Fluidized carbon particles were placed in the reactor in contact with the fuel cell anode, and helium was used to flu-

idize the carbon particles in the reactor column. The maximum power density achieved was approximately  $22 \text{ mW cm}^{-2}$  at  $900^\circ\text{C}$ . By changing Ni/YSZ and helium gas into Ni/ceria and  $\text{CO}_2$ , respectively, a power density of  $43 \text{ mW cm}^{-2}$  at  $0.5 \text{ V}$  and  $900^\circ\text{C}$  was achieved.<sup>[39]</sup> Liu et al.<sup>[40]</sup> filled carbon black into a Ni/YSZ, anode-supported, tubular SOFC with a Ni/ScSZ anode functional layer. The fuel cell achieved the maximum power densities of 104, 75 and  $47 \text{ mW cm}^{-2}$  at 850, 800 and  $750^\circ\text{C}$ , respectively, using  $\text{N}_2$  as the fluidizing gas. Gür et al.<sup>[41]</sup> further improved the performance of fluidized-bed CF-SOFCs using a Ni/YSZ cermet, anode-supported, tubular CF-SOFC at  $850^\circ\text{C}$  with  $\text{CO}_2$  as the fluidizing gas. A minimally fluidized bed of low-sulfur (0.15 wt%) Alaska coal was gasified at  $930^\circ\text{C}$  by flowing  $\text{CO}_2$  to generate CO. The highest cell power density achieved was  $450 \text{ mW cm}^{-2}$  at  $0.64 \text{ V}$  with a 35.7% electrical conversion efficiency based on CO utilization. After performance tests, the SOFC anodes were visually examined, and no significant signs of carbon deposition (i.e., coking) were observed. Independent tests in similar cells performed under galvanostatic conditions in flowing pure CO also indicated long-term stability of these anode-supported SOFC cells with no sign of degradation over several hundred hours of operation.<sup>[42]</sup>

The superiority of using  $\text{CO}_2$  as the fluidizing gas was also demonstrated in CF-SOFCs with other cermet anodes. Kakkilidis et al.<sup>[43]</sup> used lignite coal as a fuel in a tubular, YSZ-supported CF-SOFC with a Co/ $\text{CeO}_2$  anode. The influences of several parameters related to the anodic electrode composition (20, 40 and 60 wt.% Co/ $\text{CeO}_2$ ), cell temperature ( $700\text{--}800^\circ\text{C}$ ), fluidizing gas composition, and total feed flow rate ( $10\text{--}70 \text{ cm}^3 \text{ min}^{-1}$ ) were systematically examined. The optimum performance of  $\approx 10 \text{ mW cm}^{-2}$  at  $800^\circ\text{C}$  was achieved by using 20 wt.% Co/ $\text{CeO}_2$  as the anodic electrode and pure  $\text{CO}_2$ , which was found to perform better than when He was used as the fluidizing gas. Kulkarni et al.<sup>[44]</sup> used a 20-mol% yttria-doped ceria anode (YDC20) infiltrated with Ni as an anode of an electrolyte-supported fuel cell with pure unprocessed coconut char as a fuel in button CF-SOFCs, which delivered a power density of  $40 \text{ mW cm}^{-2}$  using  $\text{CO}_2/\text{N}_2$  as the fluidizing gas at  $800^\circ\text{C}$ , while the power density was  $33 \text{ mW cm}^{-2}$  with  $\text{N}_2$ . In a pure  $\text{N}_2$  atmosphere, Warburg-type diffusion dominated the cell performance due to the limited concentration of CO.

### 3.1.2. Cermet + Catalyst-Infiltrated Carbon

The literature reports that power densities of  $40\text{--}300 \text{ mW cm}^{-2}$  are possible when using a solid carbon pellet as a consumable anode or when using a traditional Ni-YSZ anode with solid carbon fuels. However, power densities in the upper region of this range can be attributed to the generation of CO in situ in the anode chamber via the reverse-Boudouard reaction and the subsequent oxidation of CO at TPBs. The CF-SOFC anode reaction mechanism has been proposed and shown to involve a two-reaction cycle: the electrochemical oxidation of CO at the anode [Reaction (8)], and the Boudouard reaction of the carbon fuel [Reaction (9)]. Solid carbon fuels are readily transported to TPB by this CO shuttle mechanism,<sup>[45]</sup> therefore, the

reciprocal coupling Reactions (8) and (9) are the key anode reactions that dominate CF-SOFC performance. It has been proven that catalysts can be added into the solid carbon to improve these two reactions effectively.

It has been widely demonstrated that alkali metal salts and iron catalysts are highly active catalysts for coal gasification.<sup>[46–53]</sup> Tang et al.<sup>[54]</sup> fabricated and tested tubular, electrolyte-supported fuel cells that were directly operated on carbon fuel. Gadolinia-doped ceria (GDC)/Ag was used as the anode, and an Fe-based catalyst was loaded into the carbon fuel to enhance the Boudouard reaction. The fuel of the Fe-loaded activated carbon was prepared by impregnation with a mass ratio of Fe:C = 1:4. The performance was shown to be significantly improved with a maximum power density of  $45 \text{ mW cm}^{-2}$  at  $800^\circ\text{C}$ , which was 10 times higher than that of the cell without any catalyst. Impedance measurements showed that the polarization resistance was decreased by at least an order of magnitude when catalysts were used in the cell. Xie et al.<sup>[55]</sup> used Ag/GDC cermet as the anode and 5-wt% Fe-loaded activated carbon as the fuel. The electricity and CO could be cogenerated in the CF-SOFCs via the electrochemical oxidation of CO and the Boudouard reaction. The rapid rate of the Boudouard reaction is necessary to achieve high electrical power and CO production. Using the emitted CO as part of the power output, an overall efficiency of 76.5% for the single cell and 72.5% for the stack was obtained. The output power density of the single cell using activated carbon as fuel was  $320 \text{ mW cm}^{-2}$  (Figure 3), which was marginally lower but comparable to that produced when using hydrogen as fuel ( $350 \text{ mW cm}^{-2}$ ).

Yu et al. showed that a potassium salt catalyst at a mass ratio of K:C = 1:10 increased the rate of carbon gasification, resulting in a significantly higher power density. The power density of CF-SOFCs with potassium carbonate infused in the carbon bed was approximately five times higher than that without a catalyst.<sup>[56]</sup>

By combining alkali metal salts and iron as the catalysts, the performance of the fuel cell could be further improved. Wu

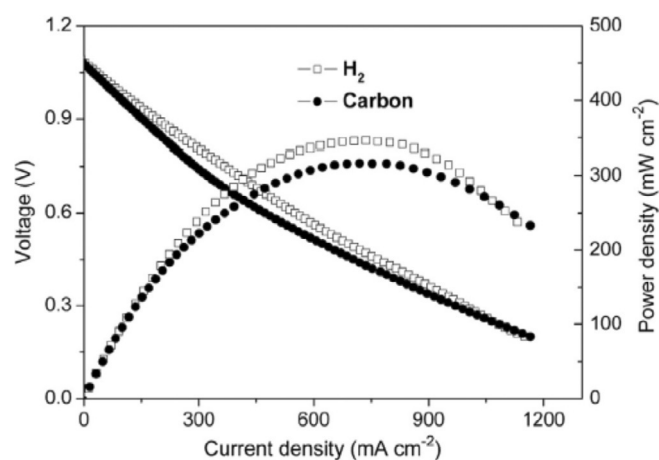


Figure 3. Typical I–V–P characteristics for the single cell operated at  $800^\circ\text{C}$  using humidified hydrogen and 5 wt% Fe-loaded carbon as fuel, respectively.<sup>[55]</sup>

et al.<sup>[57]</sup> reported a significantly improved power output from a CF-SOFC by integrating it with an in situ, catalytic, reverse-Boudouard reaction. The fuel cell used in this study was a NiO (60 wt%) + ScSZ (40 wt%), anode-supported, thin-film,  $(\text{Sc}_2\text{O}_3)_{0.1}-(\text{ZrO}_2)_{0.9}$  (ScSZ) electrolyte cell with a LSM cathode. Using an  $\text{Fe}_m\text{O}_n$ -alkaline metal oxide ( $\text{M}_x\text{O}$ ) catalyst, where  $\text{M}_x\text{O}$  was a mixture of  $\text{Li}_2\text{O}$ ,  $\text{K}_2\text{O}$  and  $\text{CaO}$ , the solid carbon was internally gasified by reacting it with  $\text{CO}_2$ . A peak power density as high as  $297 \text{ mW cm}^{-2}$  could be achieved at  $850^\circ\text{C}$  using this process, which is only modestly lower than that achieved with gaseous hydrogen as the fuel, making this system promising for use in practical applications. Jiao et al.<sup>[58]</sup> found coal char to be a more suitable fuel for CF-SOFCs compared to those using activated carbon. Loading coal char with  $\text{Fe}_m\text{O}_n$ -alkaline metal oxide catalysts further improved its reactivity and electrochemical performance. The peak power densities of the pure and catalyst-loaded coal char were approximately 100 and  $204 \text{ mW cm}^{-2}$ , respectively, at  $850^\circ\text{C}$ .

In CF-SOFCs,  $\text{CO}_2$  is formed at the anode and then reacts with the carbon fuel to form gaseous  $\text{CO}$ , which can diffuse quickly to the electrodes and thus enhance the reaction rates. However, to obtain high energy densities,  $\text{CO}_2$  must be separated from  $\text{CO}$ . Yang et al.<sup>[59]</sup> reported a novel structure for a CF-SOFC that was integrated with a ceramic  $\text{CO}_2$ -permeable membrane; this design is called a carbon-air battery. As shown in Figure 4, an anode-supported, tubular CF-SOFC functioned as a carbon fuel container as well as an electrochemical device for power generation, while a high-temperature  $\text{CO}_2$ -permeable membrane composed of a  $\text{CO}_3^{2-}$  mixture and an  $\text{O}^{2-}$  conducting phase SDC was integrated for the in situ separation of  $\text{CO}_2$  (i.e., the electrochemical product) from the anode chamber, delivering a high fuel-utilization efficiency. After modifying the carbon fuel with a reverse-Boudouard reaction catalyst to promote in situ gasification of carbon to  $\text{CO}$ , a high peak power density of  $279.3 \text{ mW cm}^{-2}$  was achieved for the battery at  $850^\circ\text{C}$ , and a small stack composed of two batteries could be operated continuously for 200 min. That study reported on the design of a novel type of electrochemical energy device that has a wide range of potential applications.

### 3.1.3. Mixed Ionic and Electronic Conductor + Carbon

It is difficult for the solid fuel to transport to the anode reaction zone or TPBs through porous anodes. Using a mixed ionic and electronic conducting (MIEC) material as the anode could facilitate the direct electrochemical reaction on the surface of the anode itself, as shown in Figure 5, without requiring the carbon to diffuse through the porous electrode to the TPBs at the electrode/electrolyte interface.<sup>[60]</sup> Over the past decade, a number of MIEC anodes have been investigated for use in hydrocarbon-based SOFCs that are resistant to coking and tolerant to impurities in hydrocarbons.<sup>[61–63]</sup> Among these anodes, titania- and ceria-based materials are particularly promising. Ceria-based anodes possess good catalytic activities and oxygen storage capacities; however, their electronic conductivities are typically low.

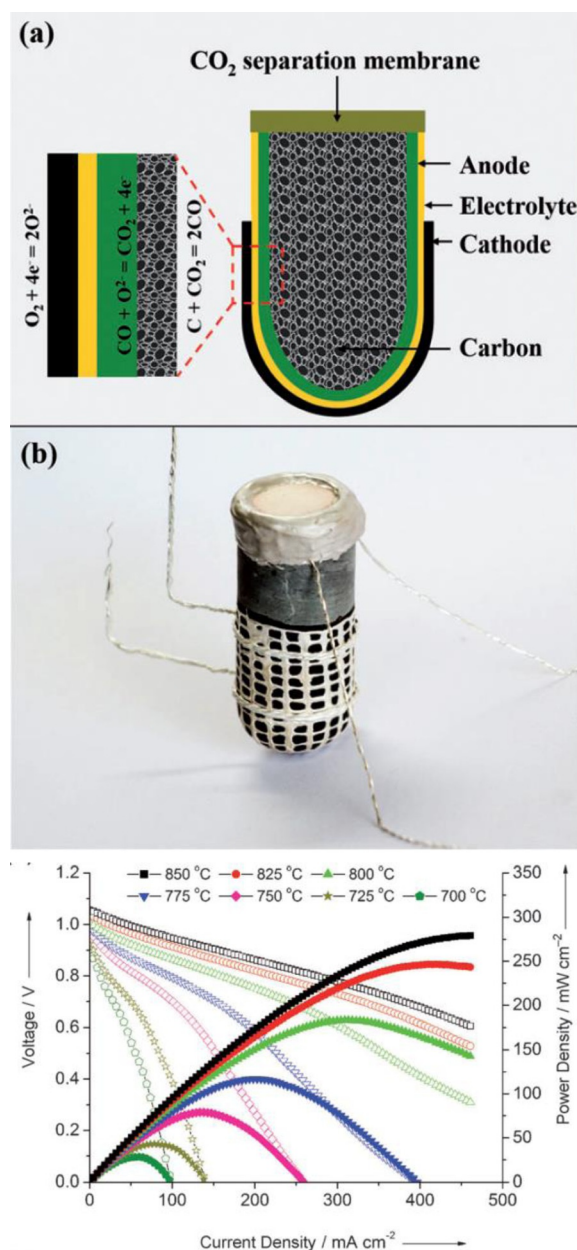


**Figure 4.** a) Diagram and b) photograph of the carbon-air battery. c)  $I$ - $V$  and  $I$ - $P$  curves of the carbon-air battery operating with activated carbon at various temperatures.<sup>[59]</sup>

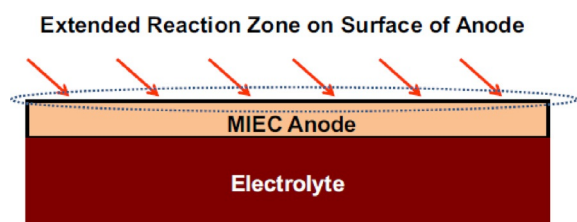


**Figure 5.** A schematic representation of the surface reaction zone in MIEC materials as the anode of a CF-SOFC.<sup>[60]</sup>

Kulkarni et al.<sup>[60]</sup> evaluated the performance of  $\text{La}_{0.6}\text{Sr}_{0.4}\text{Co}_{0.2}\text{Fe}_{0.8}\text{O}_{3-\delta}$  (LSCF) as a first-generation, mixed-con-

duction anode material. LSCF offers excellent electronic and ionic conductivities in air and is a well-known cathode material for SOFCs. When LSCF was used both as the anode and cathode in a CF-SOFC, a power density of  $50 \text{ mW cm}^{-2}$  was obtained at  $804^\circ\text{C}$  in an electrolyte-supported, small button cell that used solid carbon as the fuel. The concept of using the same anode and cathode material has also been evaluated in electrolyte-supported, thick-walled, tubular cells where a power density of approximately  $25 \text{ mW cm}^{-2}$  was obtained with carbon fuel at  $820^\circ\text{C}$  in the presence of helium as the purging gas. Although the validity of the continuous operation of this type of system was demonstrated in that study, the power densities achieved were low due primarily to the high ohmic losses in the cell, which resulted partly from the low electronic conductivity of the LSCF anode in reducing environments.<sup>[60]</sup> The electronic conductivities of LSCF bars sintered at  $1300^\circ\text{C}$  have been reported to be as low as  $1 \text{ S cm}^{-1}$  in  $\text{CO}$ .<sup>[60]</sup> These values are expected to be even lower in the porous LSCF electrodes used as anodes. To improve the electronic conductivity of the LSCF anode and for better current collection and distribution, Giddey et al.<sup>[64]</sup> investigated LSCF-Ag composites anode. Ag was added to increase the lateral conductivity of the anode and reduce ohmic losses; this design produced a 60% improvement in the power density compared to the LSCF anode.

Kulkarni et al.<sup>[65]</sup> investigated  $\text{La}_{0.3}\text{Sr}_{0.7}\text{Ti}_{0.93}\text{Co}_{0.07}\text{O}_3$  (LSCT) as a potential anode for use in a CF-SOFC that delivered a power density of  $25 \text{ mW cm}^{-2}$ . The conductivity of LSCT reached  $18 \text{ S cm}^{-1}$  in a  $\text{CO}$  atmosphere at  $800^\circ\text{C}$ . B-site doping of LST with Co was found to improve the electrical conductivity and the catalytic activity under a reducing atmosphere.

### 3.1.4. Anode + Direct Contact with Carbon

#### 3.1.4.1. Non-Porous Anode + Carbon

The direct conversion of a solid fuel on a solid electrolyte (e.g., YSZ) typically exhibits poor performance due to poor point-like contact between the two solid materials. Additionally, carbon fuel must be in close contact with the anode material, and the active area is limited to the geometric surface area. For gaseous fuels, a porous electrode is required with at least 2–3 orders of magnitude increased surface compared to a flat electrode. Because the particle density in solid carbon is approximately three orders of magnitude higher than the particle density of a gaseous fuel, a smaller active contact area could be overcompensated.<sup>[66]</sup>

Nürnberg et al.<sup>[36]</sup> show that for a system with an YSZ electrolyte, which suffers from limited contact between the solid fuel and the solid electrolyte, significant conversion rates can be achieved at such interfaces. The experimental setup is shown schematically in Figure 6. The used cells have no special anode layer; the carbon is in direct contact with the flat electrolyte surface. The principal aspects of the direct electrochemical conversion of carbon powders in an SOFC system have been investigated between  $800$  and  $1000^\circ\text{C}$ . It has been shown that when a flat planar anode is used, carbon conver-

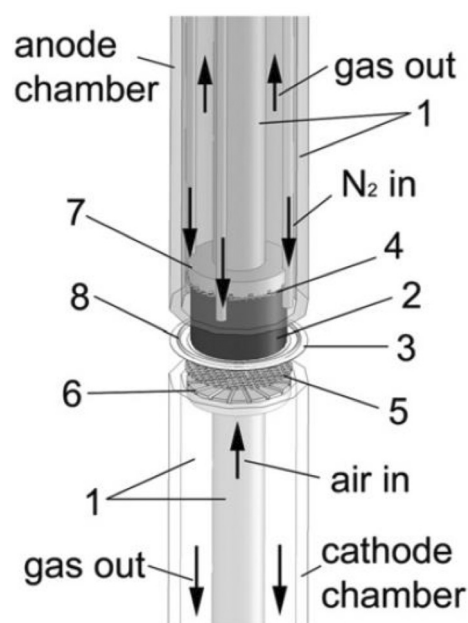


**Figure 6.** Schematic drawing of a CF-SOFC without a porous anode. 1) aluminium oxide tubes, 2) carbon pellet, 3) YSZ electrolyte, 4) current collector mesh (Ni), 5) current collector mesh (Pt), 6) cathode flow field, 7) anode flow field, 8) gold wire.<sup>[36]</sup>

sion rates exceeding  $100 \text{ mA cm}^{-2}$  are possible. Comparing this value with the total mass of the initial carbon pellet indicates that only 60% of the fuel is oxidized electrochemically; the remainder of the carbon is likely converted into  $\text{CO}$ , which has been detected in the exhaust gas stream, via the Boudouard reaction. To avoid fuel loss caused by  $\text{CO}$  formation via the Boudouard reaction, lower operating temperatures (e.g.,  $600$  to  $700^\circ\text{C}$ ) should generally be used, which, for example, could be achieved by using a modified GDC as the electrolyte.

#### 3.1.4.2. Anode + Deposited Carbon

Ihara and co-workers<sup>[67–70]</sup> proposed a rechargeable CF-SOFC that differed fundamentally from the detached or physical-contact designs with deposited carbon as the fuel. The deposited carbon was supplied via the thermal decomposition of propane or methane at the anode. In this case, the carbonaceous fuel deposited in the porous anode would be in contact with the ionic conductor, the electron conductor or the three-phase boundary.

Li et al.<sup>[71]</sup> investigated the effects of the contact type between the anode and the carbonaceous fuel on the fuel cell's reaction characteristics. The electrochemical behavior was measured for three contact types, as shown in Figure 7: detached fuel, fuel in physical contact with the anode, and carbon-deposited contact. The carbon-deposited-type fuel cell showed the best performance with a significant activation polarization due to the electrochemical oxidization of the deposited carbon. For the physical-contact-type fuel cell, the anode reaction mechanism is the same as for the detached-fuel-type fuel cell with no electrochemical reactions that involve the carbon

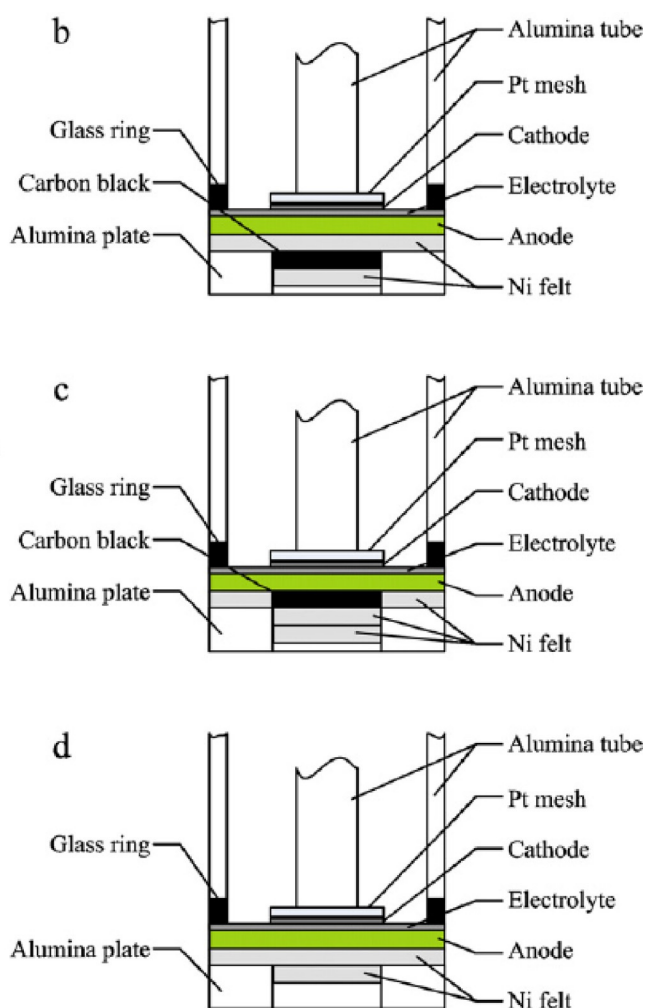


Figure 7. Schematics of the test setup for the various contact type in CF-SOFCs, including a) detached, b) physical contact and c) carbon-deposited.<sup>[71]</sup>

at the physical contact interface between the carbonaceous fuel and the anode; thus, increased physical contact does not improve cell performance. For the detached-fuel-type fuel cell, the reaction characteristics closely depend on the anode gas. The primary anode reactions are the electrochemical reaction to produce  $O_2$ ; carbon gasification with the formed  $O_2$  or with  $CO_2$ ; the electrochemical oxidation of the formed CO in a  $CO_2$  atmosphere.

Li et al.<sup>[72]</sup> investigated  $CH_4$ -deposited carbon at the anode as a fuel in CF-SOFCs. The results of that study indicate that all of the carbon deposited onto the YSZ particle surfaces, the Ni particle surfaces and TPB could participate in the electrochemical reactions during fuel-cell discharging. Lee et al.<sup>[73]</sup> found that the TPBs of Ni-YSZ conducts the electrochemical reactions even when surface of Ni was deactivated by deposited carbon. The electrochemical reactions for the deposited carbon are most difficult on the Ni particle surfaces, easier on the YSZ particle surfaces and easiest at TPB.

## 3.2. Melton Carbonates Anode

### 3.2.1. Molten Carbonates + Carbon

To improve the degree of contact between the solid fuel and oxidation species, molten salts are used in the anode chamber of a CF-SOFC. The introduction of the molten salt brings the solid carbon to the interface of the electrode and electrolyte, thus extending the reaction zone from two dimensions to three dimensions, improving the cell performance. Various concepts have been proposed to develop carbon fuel cells using molten salts and solid oxide electrolytes. The first type of carbon fuel cell was developed based on molten alkali hydroxides, while the hydroxide is subject to degradation via a reaction with carbon dioxide.<sup>[27,32,33]</sup> Replacement of hydroxide with carbonate salts mitigates any electrolyte degradation. This design is different from a molten carbonate fuel cell (MCFC) that uses carbon fuel, which require the introduction of  $CO_2$  at the cathode, complicating the balance of the plant (BOP), while molten carbonate CF-SOFCs contain a solid electrolyte to separate the molten carbonate and oxidation gas, eliminating the need to recirculate the  $CO_2$  (Figure 8).<sup>[74]</sup> Molten carbonate

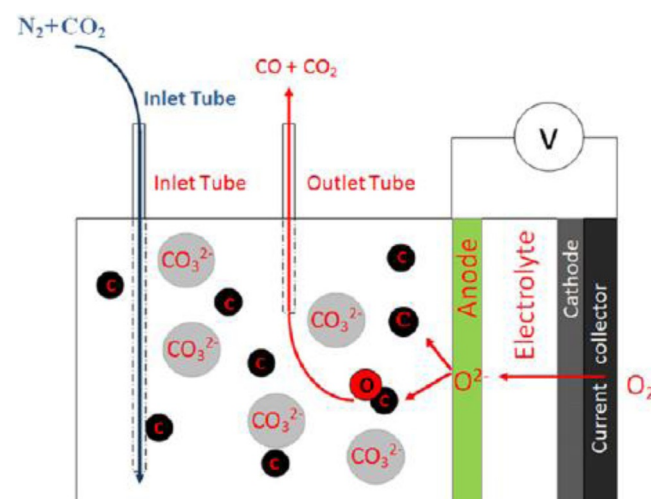


Figure 8. Schematic configuration of a molten carbonate CF-SOFC.<sup>[74]</sup>

CF-SOFC, which are also known as HDCFCs, were first proposed by Peelen et al. (1998).<sup>[75]</sup> The most developed molten carbonate CF-SOFC was produced by SRI<sup>[76]</sup> and consisted of a YSZ electrolyte that separated a molten Ag cathode from a ternary eutectic alkali (Li, Na and K) carbonate melt anode containing dispersed carbon  $[C-(Li/K/Na)_2CO_3 | YSZ | Ag(l)]$  that operated between 700 and 950 °C.<sup>[77]</sup>

Important advances in molten carbonate CF-SOFC technology were reported when pyrolyzed medium-density fiberboard (*p*-MDF) and activated carbon fuels were used with planar button cells made of NiO/YSZ/YSZ-LSM materials and a eutectic lithium/potassium molten carbonate. Power densities of 50 and 394  $mW\text{ cm}^{-2}$  were demonstrated using electrolyte- and anode-supported cells, respectively, with OCV of 1.15–1.23 V.<sup>[78–80]</sup> Chien et al.<sup>[26]</sup> studied the scale-up of molten car-

bonate CF-SOFCs via the design and testing of a single-stack repeat unit with realistic cell sizes. A single cell with a  $12.56 \text{ cm}^2$  active area produced a maximum power of approximately  $1.2 \text{ W}$  at  $800^\circ\text{C}$  and a current density of  $200 \text{ mA cm}^{-2}$  at  $0.6 \text{ V}$  using *p*-MDF as a fuel. In comparison, a fuel cell that used activated carbon as a fuel produced a maximum power density of  $36$  and  $53 \text{ mW cm}^{-2}$  at  $700$  and  $800^\circ\text{C}$ , respectively, and an electrical efficiency of approximately  $40\%$  evaluated below  $0.7 \text{ V}$  for  $17 \text{ h}$  at  $700^\circ\text{C}$ . These results demonstrated the applicability of molten carbonate CF-SOFC to practical systems, while stack units were operated in batch mode, and an appropriate fuel feeding mechanism had to be designed.

Recently reported molten carbonate CF-SOFCs are typically operated above  $700^\circ\text{C}$ . High operating temperatures may lead to the occurrence of the reverse-Boudouard reaction, which may decrease fuel efficiency. The problem of anode corrosion still remains. It has been suggested that reducing the operating temperature of the fuel cells can minimize the reverse-Boudouard reaction and certain material corrosion issues. Other benefits, such as rapid startup and cool-down cycles as well as less expensive materials for cell fabrication, can also be achieved by reducing operating temperatures to  $700^\circ\text{C}$  or below. However, molten carbonate CF-SOFCs exhibited poor performance at lower temperature due to the high resistance of solid carbon oxidation at the anode;<sup>[78–83]</sup> the anode resistance can exceed tens of  $\Omega \text{ cm}^2$ . Jiang et al. reported an anode-supported molten carbonate CF-SOFC that delivered an exciting high peak power density of  $878 \text{ mW cm}^{-2}$  at  $750^\circ\text{C}$ .<sup>[79]</sup> The high performance of that design was ascribed to the reduced thickness of the electrolyte. However, the resistive loss from the anode side was  $0.5 \Omega \text{ cm}^2$  at  $750^\circ\text{C}$ , which can be even larger at lower temperatures. Therefore, the anode resistance in fuel cells must be reduced to improve their performance further. Xu et al.<sup>[84]</sup> reported a high-performance,  $\text{Sm}_{0.2}\text{Ce}_{0.8}\text{O}_{1.9}$  (SDC) electrolyte-supported, molten carbonate CF-SOFC with a  $\text{Ba}_{0.5}\text{Sr}_{0.5}\text{Co}_{0.8}\text{Fe}_{0.2}\text{O}_{3-\delta}$  cathode and an optimized anode configuration. The catalytic oxidation of carbon was shown to be improved with that system, resulting in an area-specific resistance of only  $0.41 \Omega \text{ cm}^2$  at  $650^\circ\text{C}$  at the anode. That fuel cell design achieved a peak power density of  $113.1 \text{ mW cm}^{-2}$  at  $650^\circ\text{C}$  when activated carbon was used as a fuel. The stability of the fuel cell has also been improved due to optimized current collection. The performance of the anode can be enhanced by infiltrating nano-sized Ni into the YSZ scaffold for SOFCs operating on gas fuels. The authors attempted to enhance the performance of the fuel cells by using an infiltrated Ni/SDC anode. However, lower peak power ( $36.0 \text{ mW cm}^{-2}$ ) and current densities ( $163.1 \text{ mA cm}^{-2}$ ) were obtained at  $650^\circ\text{C}$ . The infiltrated Ni particles were found to have a detrimental effect on cell performance due to the block effect of Ni particles. To identify the function of Ni in this system, a blank, porous, SDC anode without Ni catalysts was investigated and was found to produce a peak power density of  $40.5 \text{ mW cm}^{-2}$ . Figure 9 shows the schematics of the transport of oxygen ions through three different anodes of molten carbonate CF-SOFCs. The oxygen ions produced in the cathode move through the

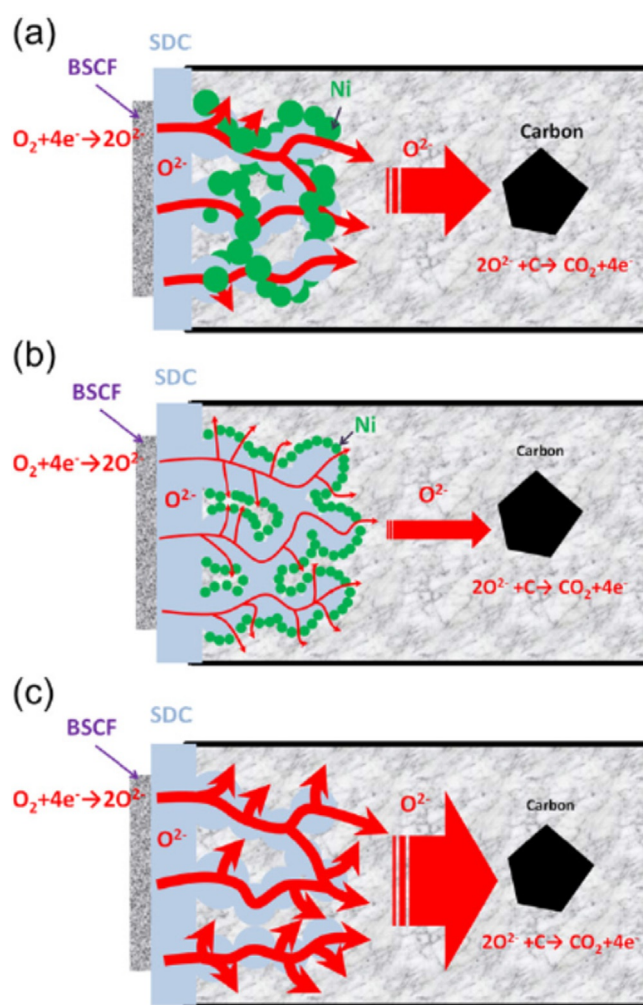


**Figure 9.** Schematics of the oxygen ions transport through three different anodes of the molten carbonate CF-SOFCs: a) tape-casted Ni/SDC, b) pasted Ni infiltrated SDC, and c) blank porous SDC.<sup>[84]</sup>

SDC electrolyte to the SDC–carbonate interface and then make contact with the molten carbonates. The carbon fuel is solid and has larger particle sizes (e.g.,  $> 20 \mu\text{m}$ ), so it is restricted from entering the pores of the Ni/SDC anode. The oxidation of carbon can occur in the molten carbonates due to the high ionic conductivity of the molten carbonates. Therefore, Ni catalysts lose their catalytic function when a porous anode is used. The Ni on the SDC surface may block the diffusion of oxygen ions at the SDC–carbonates interface. The infiltrated Ni particles can cover the SDC more uniformly than Ni particles that have been sprayed on, which can reduce anode performance even further.

Lee et al.<sup>[85]</sup> investigated the effect of anode microstructure on molten carbonate CF-SOFC performance and proposed an effective method to improve the power capability of these types of SOFCs. Poly(methyl methacrylate) (PMMA) particles were used to form pores of various sizes in a Ni-YSZ anode and thus to modify the anode microstructure (i.e., pore volume and surface area). The polarization behaviors of molten carbonate CF-SOFCs were examined using anodes with three

different microstructures and were analyzed to establish a relationship between the anode microstructure and electrochemical performance. The results showed that the incorporation of PMMA-derived pores in the anode leads to an increased power density under typical operating conditions. It was also recognized that the anode surface area is important to the performance of the system. The oxygen ions transport through the electrolyte-molten carbonates interface is similar to the rate-determining step in the anode reaction; increasing the area of the electrolyte-molten carbonates interface is critical to improving cell performance.

### 3.2.2. Molten Carbonates + Additives + Carbon

Deleebecq et al. added<sup>[86]</sup> silver oxide ( $\text{Ag}_2\text{O}$ ) as an additive to a molten medium composed of solid carbon black and  $(\text{Li-K})_2\text{CO}_3$  that was placed in contact with a Ni-YSZ anode.  $\text{Ag}_2\text{O}$  showed a high catalytic activity between 700 and 800 °C in a mixed  $\text{N}_2$ - $\text{CO}_2$  anode atmosphere during a test based on thermo-gravimetric differential thermal analysis (TGA-DTA). Using this additive, the fuel cells showed improved electrochemical performance compared to the addition of powdered metallic silver metal (Ag),  $\text{Ag}_2\text{CO}_3$  and a blank cell because  $\text{Ag}_2\text{O}$  promoted carbon gasification and CO oxidation.

Lee et al.<sup>[87]</sup> found that the performance of MCFC-carbon fuel cells could be improved by increasing wettability with the addition of  $\text{Gd}_2\text{O}_3$  to the molten carbonates. The peak power density was found to linearly increase with the proportion of  $\text{Gd}_2\text{O}_3$  addition from 60.05  $\text{mWcm}^{-2}$  for the simple Ni anode to 106.76  $\text{mWcm}^{-2}$  for the Ni: $\text{Gd}_2\text{O}_3 = 1:5$  anode. These results imply that the addition of  $\text{Gd}_2\text{O}_3$  had a significant influence on the electrochemical activity. Significant performance enhancements were also observed with the addition of  $\text{CeO}_2$  in graphite anode by Liu et al.<sup>[88]</sup> The improvement in activity by adding  $\text{CeO}_2$  was proposed to provide indirect oxidation pathways by allowing the released electrons to move through ceria reduced by graphite following electro-oxidation or chemical oxidation with generation of CO, which is then electro-oxidized. The indirect electro-oxidation of graphite occurs and works together with direct reactions, contributing to improved performance. It is reasonable to expect that such a strategy is also helpful in improving the performance of the molten carbonate CF-SOFCs.

### 3.3. Molten Metals Anode

Although molten carbonates exhibit high ionic conductivities at elevated temperatures, they are poor electrical conductors that limit the performance of these cells. One of the most promising methods uses molten metal as the anode electrode, which exhibits good oxygen conductivity and a high electrical conductivity.

Yentekakis et al.<sup>[89]</sup> designed a fuel cell that used a molten iron bath as the anode in 1989. In this fused metal-YSZ-platinum- $\text{O}_2$  design, fine carbon is fed into the fused iron anode as fuel, and air is fed into the cathode. The design shows promising performance; however, it introduces many challenges be-

cause the fuel cell must be operated above the melting point of iron (1536 °C). CellTech Power LLC (CellTech) developed a layer of liquid tin as the anode to directly convert carbonaceous fuels including coal into electricity without gasification at 800–1000 °C.<sup>[90,91]</sup> A solid  $\text{SnO}_2$  layer formed at the electrolyte interface was observed during fuel cell operation at 700 °C; this layer inhibits the further transfer of the oxygen from the tin-electrolyte interface, resulting in high anode losses. To mitigate the effects of this oxide layer, operation above 1000 °C is suggested because  $\text{SnO}_2$  formation is thermodynamically unfavorable at this temperature. This high temperature is also required for cell operation due to the relatively high impedances exhibited in liquid-Sn anode cells.<sup>[92,93]</sup> Sn can also be used as a mediator on a Ni-YSZ anode surface to promote the oxidation of carbon,<sup>[94]</sup> electricity is then generated by carbon, which is used as an electrochemically oxidizable fuel, not by the liquid Sn. Jang et al.<sup>[95]</sup> investigated the catalytic effect of Sn as a mediator on a Ni-YSZ anode surface. The addition of 15 mg of Sn showed the best performance with a maximum power density of 136  $\text{mWcm}^{-2}$  at 850 °C, while 60 mg of Sn covered the Ni-YSZ anode surface and pores too thickly and thus hindered the carbon's access to the TPBs, leading to a relatively low power density. The model experiments suggest that 15–30 mg of Sn is the optimal quantity to improve the interfacial mediating effect due to its excellent distribution properties, permeation and mediation as a liquid-state Sn at higher temperatures.

Alternatively, it is critical to develop the fuel cells with molten baths. In these systems, both the metals and metal oxides should have low melting points. Jayakumar et al.<sup>[96]</sup> examined indium (In), lead (Pb), antimony (Sb), bismuth (Bi), and silver (Ag) as anodes. The electrode resistance associated with molten antimony is approximately 0.06  $\Omega\text{cm}^2$ , which produces a peak power density of 350  $\text{mWcm}^{-2}$  at 700 °C, although the calculated OCV for the Sb- $\text{Sb}_2\text{O}_3$  mixture is only 0.75 V.

Molten Ag and Ag-Sb alloy have been examined as anodes at 900 °C.<sup>[97]</sup> For Ag, an OCV that is typical of that expected for carbon oxidation (1.12 V) was observed when charcoal was mixed with the molten Ag. However, the anode impedance was found to be as high as 100  $\Omega\text{cm}^2$ . The nature of the electrode losses was investigated by measuring the voltage-current characteristics of a cell with Ag that had no carbon at the electrode, while ramping the voltage under conditions typically seen in fuel cells and during electrolysis. The results indicated that cell potential is governed by the oxygen concentration in the Ag at the electrolyte interface. Using this result and a model of carbon oxidation within molten Ag, it was shown that the impedance of the electrode is limited by the diffusion of oxygen in the Ag phase due to the low solubility of oxygen in molten Ag. With an Ag-Sb alloy with added charcoal, the OCV at 700 °C was found to be 0.75 V, which is the potential associated at equilibrium between Sb and  $\text{Sb}_2\text{O}_3$  due to the low solubility of oxygen in the Sb phase.

Electrolyte stability is an issue that should be considered when using molten antimony as an anode. Scandium-stabilized zirconia (ScSZ) was used as the electrolyte in these studies. Severe corrosion of the electrolyte in molten antimony was

found in the regions of high current flow. No corrosion was observed when YSZ was used as the electrolyte at the same current densities. However, the ionic conductivities of YSZ are one order of magnitude lower than those of ScSZ.<sup>[98]</sup> Xu et al.<sup>[99]</sup> report a high-performance, SDC electrolyte-supported CF-SOFC with a molten antimony anode because the ionic conductivities of SDC are comparable to those of scandium-stabilized zirconia. The area-specific resistances associated with the molten Sb–Sb<sub>2</sub>O<sub>3</sub> electrode were only 0.026, 0.045, and 0.121 Ω cm<sup>2</sup> at 750, 700, and 650 °C, respectively, while the maximum power outputs were 327, 268, and 222 mW cm<sup>-2</sup> at the corresponding temperatures. An SDC electrolyte thus exhibits tolerance to the corrosion of molten antimony at high temperature in the period investigated.

#### 4. Conclusions

Compared with gas-fueled SOFCs, CF-SOFCs are in their infancy but offer an incremental increase in efficiency over traditional and emerging solid-fuel combustion technologies with the added advantages of low greenhouse gas emissions, low costs and low energy requirements for carbon capture and storage. Existing CF-SOFCs can be classified into three types based on the type of the anode used: 1) solid-oxide anode; 2) molten-carbonate anode; and 3) molten-metal anode. Low power densities and short useful lifetimes are common issues with these three types of CF-SOFCs. Molten carbonate and molten metal CF-SOFCs exhibit relatively higher power densities than those use a solid-oxide anode. However, the disadvantages of molten carbonate and molten metal CF-SOFCs include severe corrosion of fuel-cell components in molten-carbonate<sup>[100]</sup> and molten-metal environments.<sup>[98]</sup> Thus, substantial research and development are required to further develop new materials and optimize the microstructure for the anodes of these types of SOFCs to improve their electrochemical performance and stability in operating environments.

**Keywords:** anodes · carbon · electrochemical energy conversion · kinetics · solid oxide fuel cells

[1] B. C. H. Steele, A. Heinzl, *Nature* **2001**, *414*, 345.  
 [2] S. M. Haile, *Acta Mater.* **2003**, *51*, 5981.  
 [3] M. Winter, R. J. Brodd, *Chem. Rev.* **2004**, *104*, 4245.  
 [4] M. Mogensen, K. Kammer, *Annu. Rev. Mater. Res.* **2003**, *33*, 321.  
 [5] Z. P. Shao, W. Zhou, Z. H. Zhu, *Prog. Mater. Sci.* **2012**, *57*, 804.  
 [6] S. McIntosh, R. J. Gorte, *Chem. Rev.* **2004**, *104*, 4845.  
 [7] D. J. L. Brett, A. Atkinson, N. P. Brandon, S. J. Skinner, *Chem. Soc. Rev.* **2008**, *37*, 1568.  
 [8] N. Q. Minh, *J. Am. Ceram. Soc.* **1993**, *76*, 563.  
 [9] M. Ni, M. K. H. Leung, D. Y. C. Leung, *Int. J. Energy Res.* **2009**, *33*, 943.  
 [10] A. Atkinson, S. Barnett, R. J. Gorte, J. T. S. Irvine, A. J. McEvoy, M. Mogensen, S. C. Singhal, J. Vohs, *Nat. Mater.* **2004**, *3*, 17.  
 [11] M. Y. Gong, X. B. Liu, J. Tremblay, C. Johnson, *J. Power Sources* **2007**, *168*, 289.  
 [12] J. B. Goodenough, Y. H. Huang, *J. Power Sources* **2007**, *173*, 1.  
 [13] S. P. Jiang, S. H. Chan, *J. Mater. Sci.* **2004**, *39*, 4405.  
 [14] X.-M. Ge, S.-H. Chan, Q.-L. Liu, Q. Sun, *Adv. Energy Mater.* **2012**, *2*, 1156.  
 [15] J. W. Fergus, *Solid State Ionics* **2006**, *177*, 1529.  
 [16] C. W. Sun, U. Stimming, *J. Power Sources* **2007**, *171*, 247.  
 [17] W. Wang, C. Su, Y. Z. Wu, R. Ran, Z. P. Shao, *Chem. Rev.* **2013**, *113*, 8104.

[18] *BP Statistical Review of World Energy*, BP, London, **2012**.  
 [19] J. E. Sinton, D. G. Fridley, *Energy Policy* **2000**, *28*, 671.  
 [20] A. C. Rady, S. Giddey, S. P. S. Badwal, B. P. Ladewig, S. Bhattacharya, *Energy Fuels* **2012**, *26*, 1471.  
 [21] P. Desclaux, S. Nurnberger, M. Rzepka, U. Stimming, *Int. J. Hydrogen Energy* **2011**, *36*, 10278.  
 [22] S. L. Jain, Y. Nabaee, B. J. Lakeman, K. D. Pointon, J. T. S. Irvine, *Solid State Ionics* **2008**, *179*, 1417.  
 [23] M. Dudek, R. I. Tomov, C. Wang, B. A. Glowacki, P. Tomczyk, R. P. Socha, M. Mosiałek, *Electrochim. Acta* **2013**, *105*, 412.  
 [24] M. Dudek, *Solid State Ionics* **2015**, *271*, 121.  
 [25] W. Z. Cai, Q. Zhou, Y. M. Xie, J. Liu, *Fuel* **2015**, *159*, 887.  
 [26] A. C. Chien, G. Corre, R. Antunes, J. T. S. Irvine, *Int. J. Hydrogen Energy* **2013**, *38*, 8497.  
 [27] T. M. Gür, *Chem. Rev.* **2013**, *113*, 6179.  
 [28] W. W. Jacques, Method of converting potential energy of carbon into electrical energy, U.S. Patent Office. Patent no. 5555111896.  
 [29] R. D. Weaver, S. C. Leach, A. E. Bayce, L. Nanis, *Direct Electrochemical Generation of Electricity from Coal*, SRI, Menlo Park, CA, 1979.  
 [30] N. J. Cherepy, R. Krueger, K. J. Fiet, A. F. Jankowaki, J. F. Copper, *J. Electrochem. Soc.* **2005**, *152*, A80.  
 [31] D. X. Cao, Y. Sun, G. L. Wang, *J. Power Sources* **2007**, *167*, 250.  
 [32] L. Delebeeck, K. K. Hansen, *J. Solid State Electrochem.* **2014**, *18*, 861.  
 [33] S. Giddey, S. P. S. Badwal, A. Kulkarni, C. Munnings, *Prog. Energy Combust. Sci.* **2012**, *38*, 360.  
 [34] K. Hemmes, J. F. Cooper, J. R. Selman, *Int. J. Hydrogen Energy* **2013**, *38*, 8503.  
 [35] G.-Y. Liu, Y.-T. Zhang, J.-T. Cai, X.-Q. Zhang, J.-S. Qiu, *New Carbon Mater.* **2015**, *30*, 12.  
 [36] S. Nurnberger, R. Bußar, P. Desclaux, B. Franke, M. Rzepka, U. Stimming, *Energy Environ. Sci.* **2010**, *3*, 150.  
 [37] T. M. Gür, R. A. Huggins, *J. Electrochem. Soc.* **1992**, *139*, L95.  
 [38] S. Li, A. C. Lee, R. E. Mitchell, T. M. Gür, *Solid State Ionics* **2008**, *179*, 1549.  
 [39] A. C. Lee, S. W. Li, R. E. Mitchell, T. M. Gür, *Electrochem. Solid-State Lett.* **2008**, *11*, B20.  
 [40] R. Liu, C. Zhao, J. Li, F. Zeng, S. Wang, T. Wen, Z. Wen, *J. Power Sources* **2010**, *195*, 480.  
 [41] T. M. Gür, M. Homel, A. V. Virkar, *J. Power Sources* **2010**, *195*, 1085.  
 [42] M. Homel, T. M. Gür, J. H. Koh, A. V. Virkar, *J. Power Sources* **2010**, *195*, 6367.  
 [43] N. Kaklidis, I. Garagounis, V. Kyriakou, V. Besikiotis, A. Arenillas, J. A. Menendez, G. E. Marnellos, M. Konsolakis, *Int. J. Hydrogen Energy* **2015**, *40*, 14353.  
 [44] A. Kulkarni, S. Giddey, S. P. S. Badwal, *J. Solid State Electrochem.* **2015**, *19*, 325.  
 [45] T. M. Gür, *J. Electrochem. Soc.* **2010**, *157*, B571.  
 [46] X. Li, C. Li, *Fuel* **2006**, *85*, 1518.  
 [47] J. Yu, F. Tian, M. C. Chow, L. J. McKenzie, C. Li, *Fuel* **2006**, *85*, 127.  
 [48] J. Wang, K. Sakanishi, I. Saito, *Energy Fuels* **2005**, *19*, 2114.  
 [49] G. Domazetis, J. Liesegang, B. D. James, *Fuel Process. Technol.* **2005**, *86*, 463.  
 [50] Y. Ohtsuka, K. Asami, *Catal. Today* **1997**, *39*, 111.  
 [51] S. Tanaka, T. Uemura, K. Ishizaki, K. Nagayoshi, N. Ikenaga, H. Ohme, T. Suzuki, *Energy Fuels* **1995**, *9*, 45.  
 [52] T. Suzuki, K. Inoue, Y. Watanabe, *Energy Fuels* **1988**, *2*, 673.  
 [53] K. Nagase, T. Shimodaira, M. Itoh, Y. Zheng, *Phys. Chem. Chem. Phys.* **1999**, *1*, 5659.  
 [54] Y. B. Tang, J. Liu, *Int. J. Hydrogen Energy* **2010**, *35*, 11188.  
 [55] Y. M. Xie, W. Z. Cai, J. Xiao, Y. B. Tang, J. Liu, M. L. Liu, *J. Power Sources* **2015**, *277*, 1.  
 [56] X. K. Yu, Y. X. Shi, H. J. Wang, N. S. Cai, C. Li, A. F. Ghoniem, *J. Power Sources* **2014**, *252*, 130.  
 [57] Y. Z. Wu, C. Su, C. M. Zhang, R. Ran, Z. P. Shao, *Electrochem. Commun.* **2009**, *11*, 1265.  
 [58] Y. Jiao, W. J. Tian, H. L. Chen, H. G. Shi, B. B. Yang, L. Chao, Z. P. Shao, Z. P. Zhu, S.-D. Li, *Appl. Energy* **2015**, *141*, 200.  
 [59] B. B. Yang, R. Ran, Y. J. Zhong, C. Su, M. O. Tade, Z. P. Shao, *Angew. Chem. Int. Ed.* **2015**, *54*, 3722; *Angew. Chem.* **2015**, *127*, 3793.  
 [60] A. Kulkarni, F. T. Ciacchi, S. Giddey, C. Munnings, S. P. S. Badwal, J. A. Kimpton, D. Fini, *Int. J. Hydrogen Energy* **2012**, *37*, 19092.

- [61] J. T. S. Irvine, in *Perovskite Oxide for Solid Oxide Fuel Cells* (Ed.: T. Ishihara), Springer, Berlin, **2009**.
- [62] P. I. Cowin, T. G. Petit, R. Lan, J. T. S. Irvine, S. Tao, *Adv. Energy Mater.* **2011**, *1*, 314.
- [63] W. Z. Zhu, S. C. Deevi, *Mater. Sci. Eng. A* **2003**, *362*, 228.
- [64] S. Giddey, A. Kulkarni, C. Munnings, S. P. S. Badwal, *J. Power Sources* **2015**, *284*, 122.
- [65] A. Kulkarni, S. Giddey, S. P. S. Badwal, G. Paul, *Electrochim. Acta* **2014**, *121*, 34.
- [66] J. Larminie, A. Dicks, *Fuel Cell Systems Explained*, Wiley-VCH, Weinheim, **2000**.
- [67] M. Ihara, K. Matsuda, H. Sato, C. Yokoyama, *Solid State Ionics* **2004**, *175*, 51.
- [68] M. Ihara, S. Hasegawa, *J. Electrochem. Soc.* **2006**, *153*, A1544.
- [69] S. Hasegawa, M. Ihara, *J. Electrochem. Soc.* **2008**, *155*, B58.
- [70] H. Saito, S. Hasegawa, M. Ihara, *J. Electrochem. Soc.* **2008**, *155*, B443.
- [71] C. Li, Y. Shi, N. Cai, *J. Power Sources* **2011**, *196*, 4588.
- [72] C. Li, Y. Shi, N. Cai, *J. Power Sources* **2011**, *196*, 754.
- [73] D. Lee, D. Kim, J. Kim, J. Moon, *Sci. Rep.* **2014**, *4*, 3937.
- [74] A. D. Bonaccorso, J. T. S. Irvine, *Int. J. Hydrogen Energy* **2012**, *37*, 19337.
- [75] W. H. A. Peelen, K. Hemmes, J. H. W. de Wit, *High Temp. Mater. Processes* **1998**, *2*, 471.
- [76] R. H. Wolk, S. Lux, S. Gelber, F. H. Holcomb, *Direct Carbon Fuel Cells: Converting Waste to Electricity*, U.S. Army Corps of Engineers, ERDC-CERL Fuel Cell Program, September 2007.
- [77] A. S. Lipilin, I. I. Balachov, L. H. Dubois, A. Sanjurjo, M. C. McKubre, S. Crouch-Baker, M. D. Hornbostel, F. L. Tanzella, *Liquid Anode Electrochemical Cell*, USA patent, US 2007/0269688 A1, **2007**.
- [78] Y. Nabae, K. D. Pointon, J. T. S. Irvine, *Energy Environ. Sci.* **2008**, *1*, 148.
- [79] C. Jiang, J. Ma, A. D. Bonaccorso, J. T. S. Irvine, *Energy Environ. Sci.* **2012**, *5*, 6973.
- [80] K. Hemmes, M. Cassir, *J. Fuel Cell Sci. Technol.* **2011**, *8*, 051005.
- [81] S. L. Jain, J. B. Lakeman, K. D. Pointon, J. T. S. Irvine, *J. Fuel Cell Sci. Technol.* **2007**, *4*, 280.
- [82] Y. Nabae, K. D. Pointon, J. T. S. Irvine, *J. Electrochem. Soc.* **2009**, *156*, B716.
- [83] C. Jiang, J. T. S. Irvine, *J. Power Sources* **2011**, *196*, 7318.
- [84] X. Y. Xu, W. Zhou, F. L. Liang, Z. H. Zhu, *Int. J. Hydrogen Energy* **2013**, *38*, 5367.
- [85] J.-Y. Lee, R.-H. Song, S.-B. Lee, T.-H. Lim, S.-J. Park, Y. G. Shul, J.-W. Lee, *Int. J. Hydrogen Energy* **2014**, *39*, 11749.
- [86] L. Deleebeeck, D. Ippolito, K. Kammer Hansen, *Electrochim. Acta* **2015**, *152*, 222.
- [87] E.-K. Lee, H. H. Chun, Y.-T. Kim, *Int. J. Hydrogen Energy* **2014**, *39*, 16541.
- [88] J. Liu, K. Ye, K. Cheng, G. Wang, J. Yin, D. X. Cao, *Electrochim. Acta* **2014**, *135*, 270.
- [89] I. V. Yentekakis, P. G. Debenedetti, B. Costa, *Ind. Eng. Chem. Res.* **1989**, *28*, 1414.
- [90] W. A. G. McPhee, L. Bateman, M. Koslowski, M. Slaney, Z. Uzep, J. Bentley, T. Tao, *J. Fuel Cell Sci. Technol.* **2011**, *8*, 041007.
- [91] H. Abernathy, R. Gemmen, K. Gerdes, M. Koslowski, T. Tao, *J. Power Sources* **2011**, *196*, 4564.
- [92] A. Jayakumar, J. M. Vohs, R. J. Gorte, *Ind. Eng. Chem. Res.* **2010**, *49*, 10237.
- [93] W. A. G. McPhee, M. Boucher, J. Stuart, R. S. Parnas, M. Koslowski, T. Tao, B. A. Wilhite, *Energy Fuels* **2009**, *23*, 5036.
- [94] J.-H. Myung, S.-D. Kim, T. H. Shin, D. Lee, J. T. S. Irvine, J. Moon, S.-H. Hyun, *J. Mater. Chem. A* **2015**, *3*, 13801.
- [95] H. Jang, J. Eom, H. Ju, J. Lee, *Catal. Today* DOI: /10.1016/j.cattod.2015.06.013.
- [96] A. Jayakumar, R. K. Ungas, S. Roy, A. Javadekar, D. J. Buttrey, J. M. Vohs, R. J. Gorte, *Energy Environ. Sci.* **2011**, *4*, 4133.
- [97] A. Javadekar, A. Jayakumar, R. Pujara, J. M. Vohs, R. J. Gorte, *J. Power Sources* **2012**, *214*, 239.
- [98] A. Jayakumar, A. Javadekar, J. Gissing, J. M. Vohs, G. W. Huber, R. J. Gorte, *AIChE J.* **2013**, *59*, 3342.
- [99] X. Y. Xu, W. Zhou, Z. H. Zhu, *Ind. Eng. Chem. Res.* **2013**, *52*, 17927.
- [100] X. Y. Xu, W. Zhou, Z. H. Zhu, *RSC Adv.* **2014**, *4*, 2398.

Manuscript received: September 26, 2015  
Accepted Article published: November 2, 2015  
Final Article published: November 13, 2015